

**Review Article***Copyright © All rights are reserved by Naveet Kaur*

# Twenty Strange Years in the World of Rock Mechanics and Engineering Geology

**Nick Barton\****Department of Rock Engineering, Nick Barton & Associates, Norway*

**\*Corresponding author:** Nick Barton, Department of Rock Engineering, Nick Barton & Associates, Norway

**Received Date:** February 10, 2025

**Published Date:** February 17, 2025

**Abstract**

Those working in the hard, to moderately hard, rocky-end of our 'geo' subjects (as opposed to our nearer-surface soil specialists) inevitably have rather more challenging site investigation tasks prior to designing and optimizing tunnelling and mining projects. The geologic complexities of jointed and sometimes faulted rock masses cannot be readily sampled and tested in the way that soil, or concrete or steel can be brought into the test laboratories. The scope and manpower needs for the myriads of site investigations, designs and constructions are huge. This is clear if we include transport tunnels for road and rail, city metro when tunnels and stations are mostly in rock, hydropower and pumped storage projects, underground and open-pit mining projects, and major dam projects in steep-walled river valleys. All of them are expensive constructions and mostly in rock. There are therefore tens of thousands of geologists, engineering geologists and rock engineers involved, and hundreds of thousands perhaps millions developing and working in the related civil engineering and mining projects. Clearly this is a trillion-dollar industry as emphasized by the reality of a recent 2.5 billion dollar claim when things went badly wrong at a major hydropower project. This article focusses on the strengths and shortcomings of methods of rock mass description and modelling of tunnels, caverns and rock slopes. It addresses in particular the problems with the Hoek-Brown GSI (geological strength index) and its widespread application in unrealistic but simply performed continuum models. These are colourful productions but are misleading our students and likely misleading the owners who pay for cut-price analyses. A radical rethink is needed if rock engineering design is to be of actual use to our numerous clients.

## Rock Mass Characterization Methods RMR, Q and GSI

Because of the difficulty of testing rock masses at sufficient scale it has been common practice for the last 50 years to use quantitative rock mass characterization methods. Following an earlier Terzaghi method for steel-arch supported tunnels that originated in the USA when steel was cheap, the three most commonly used 'western' methods (among at least 35 other proposals: Erharter et al. [1]) have been Bieniawski's RMR (rock mass rating) originating in 1973, Barton's Q-system (quality, or lack of quality) originating

in 1974, and Hoek's GSI (geological strength index) originating in 1994. RMR and GSI share a more or less equal numeric range of about 5 to 95 and have a 'joint condition' description in common, adapted from Bieniawski, 1989.

The Q-value scale by comparison stretches from 0.001 (exceptionally poor) to 1000 (exceptionally good) and is designed to more easily reflect the orders of magnitude ranges of shear strength, deformability and permeability of rock masses. According to a recent international review using several hundred respondents

from numerous countries [1] the Q-system is the most frequently used rock mass characterization method around the world for *underground projects*. It provides rock quality classes, for instance based on core-logging, and supplies tunnel and cavern support recommendations, plus some slope stability numbers used in designing large mining excavations. It has also been adapted for TBM prognosis (QTBM) and for selecting stable rock slope angles (QSLOPE). It has been simply linked to tunnel deformation, to tunnel support pressure, to the cost and duration of tunnelling, and to depth-dependent permeability, P-wave velocity, and deformability. Each of the above were summarized recently in a keynote paper with key co-authors [2].

GSI as compared to Q or RMR is an *ultra-simple* numeric characterization of the rock mass quality followed by application of the GSI rating in the *ultra-complex* Hoek-Brown equations that supposedly link GSI to the cohesive and frictional strength of rock masses if they could be simplified as isotropic continua (i.e. unjointed and unfaulted). Estimates of the apparent unconfined compressive strength of the 'continuum' rock masses and their assumed deformation modulus are also provided using GSI. Unfortunately, despite wide-spread use in many countries for the last two decades, and strong and successful marketing by a Canadian software company who have mostly specialized in FEM analyses

of continua, it turns out that the estimated rock mass quality (or geologic strength index rating GSI) is utilized a remarkable 16 times in the Hoek-Brown (Hoek et al. 2002) equation for the Mohr-Coulomb parameter 'c' (cohesion), also 12 times in the H-B equation for friction angle 'φ' and 10 times for the estimate of uniaxial strength 'σ<sub>cm</sub>'. To add to this uncertainty and ambiguity there is a disturbance factor D that appears 7 times and 6 times in the H-B equations for 'c' and 'φ'. As readers might imagine, any 'error' in the GSI estimate is inevitably amplified with this extraordinary over-use of GSI in key input data, making the subsequent numerical analyses of questionable value. Yet GSI has been used by thousands and is taught in university courses alongside RMR and Q and other subjects of rock mechanics theory and practice.

## The Distribution of Rock Mass Classification and Characterization

As will be seen when studying Figures 1a & 1b, reproduced from Erhartner et al. [1], the distribution of rock mass characterization methods is quite different for underground and surface applications. This is linked of course with the fact that Hoek's GSI does not provide tunnel support recommendations. It is instead strongly linked to providing estimates of input parameters for FEM modelling, usually for modelling tunnels or rock slopes as continua.

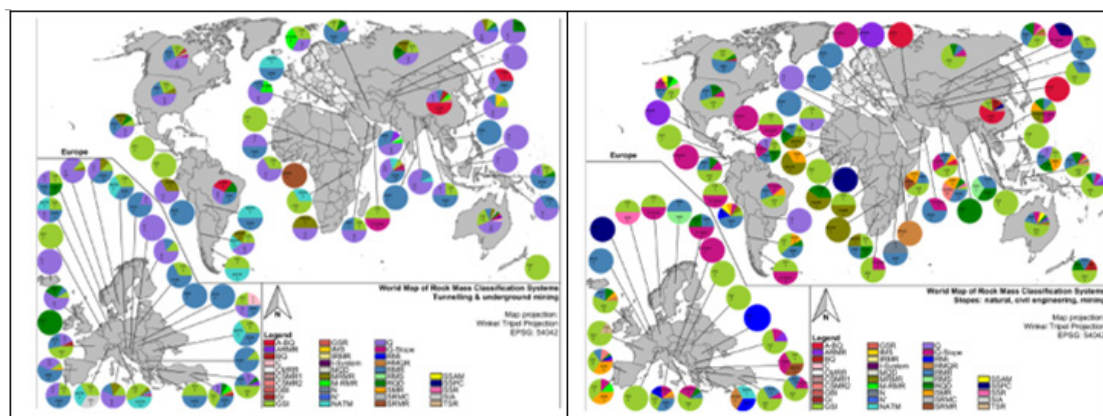


**Figure 1:** World map of frequency of application, country by country, of rock mass classification and characterization systems a) in tunnelling and underground mining, b) for slope engineering applications in mining and civil engineering. Note preponderance of purple (Q) and blue (RMR) in a), and preponderance of green (GSI) in b). Reproduced from Erhartner et al. [1].

## The Surprising Over-Exposure of GSI in Hoek-Brown Equations

It is possible to imagine that many readers think they have misunderstood what was written above, about GSI's multiple use in key equations that thousands are using in numerical models. This is because it is clearly absurd and spreads uncertainty. The writer of this article, for instance, developed a commonly used equation for the peak shear strength of rock joints [3] which includes the parameters JRC (joint roughness coefficient) and JCS (joint wall strength). These readily obtained, meaningful index numbers are used to calculate the role of joint roughness caused by the

interlock of asperities. So now imagine that the peak friction angle thus obtained (say 42°) needed JRC to appear 16 times, and JCS to appear 12 times in 'a page-wide' Barton equation for shear strength to obtain this value of 42°. The profession would not have taken any of this seriously, and the writer's 'absurd equation' would have immediately disappeared without trace fifty years ago. However, as it is in fact a simple and logical equation, it is still used in modelling, such as in Itasca's and Cundall's UDEC, known as UDEC-BB since 1985. (BB stands for Barton-Bandis: see later).

$$\tan^{-1}(T / \sigma_n) = \phi_{peak} = JRC \cdot \log_{10}(JCS / \sigma_n) + \phi_r \quad (1)$$

Note that JRC and JCS appear just once as is conventional. The Hoek-Brown equations that are proposed for estimating the stress-dependent values of 'c' and 'φ' for rock masses have an absurd level of repetition of GSI as can be seen in Figure 2. Sadly for our profession they are used by thousands who are perhaps unaware

of what is coded in rented commercial software. They just select values for:  $m_i$  s a  $\sigma_{ci}$  D GSI and confining pressure, and the software gives them input for colourful FEM stress, deformation and 'plastic zone' plots.

|   |  |  |
|---|--|--|
| $c' = \frac{\sigma_{ci} [(1+2a)s + (1-a)m_b \sigma'_{3n}] (s + m_b \sigma'_{3n})^{a-1}}{(1+a)(2+a) \sqrt{1 + (6am_b (s + m_b \sigma'_{3n})^{a-1}) / (1+a)(2+a)}}$ |  |  |
| $\phi' = \sin^{-1} \left[ \frac{6am_b (s + m_b \sigma'_{3n})^{a-1}}{2(1+a)(2+a) + 6am_b (s + m_b \sigma'_{3n})^{a-1}} \right]$                                    |  |  |
| $m_b = m_i \exp \left( \frac{GSI - 100}{28 - 14D} \right)$  | $s = \exp \left( \frac{GSI - 100}{9 - 3D} \right)$ | $a = \frac{1}{2} + \frac{1}{6} \left( e^{-\frac{GSI}{15}} - e^{-\frac{20}{3}} \right)$     |
| $\sigma'_{c,m} = \sigma_{ci} \frac{[m_b + 4s - a(m_b - 8s)](m_b / 4 + s)^{a-1}}{2(1+a)(2+a)}$   |  | $E_m (\text{MPa}) = 10^5 \left( \frac{1 - D/2}{1 + e^{\frac{75 + 25D - GSI}{11}}} \right)$ |

**Figure 2:** The third coloured line with three smaller supporting equations mean that the principal 'c' and 'φ' across-the-page-equations actually contain the chosen GSI rating a total of 16 and 12 times respectively. (Those doubting this, please check). GSI is also used 10 times in the equation for  $\sigma_{cm}$  ('UCS' for the rock mass). The equation for  $E_m$  (deformation modulus) has no adjustment for depth, and virtually any value can be obtained by varying the disturbance factor D from 0 to 1.0. This will be graphed later as it is simply extraordinary.

One can only wonder at the consequences of 'an error' in GSI (itself a very weak parameter) since it will appear 16 and 12 times in these two principal equations. Worse still, rock masses do not reach failure by the H-B assumed Mohr-Coulomb-based addition of 'c' and  $\sigma_n \tan \phi'$ . The cohesion (for instance of intact bridges between rock joints) is overcome at smaller strain than the mobilization

of 'friction which remains', as correctly stated by Müller, 1966 a long time ago. Most individuals and even software companies are continuing to make the classic modelling error of adding the 'c' and 'φ' components. This is not how jointed rock masses fail. A more correct progressive failure model (CcSs) will be shown later.

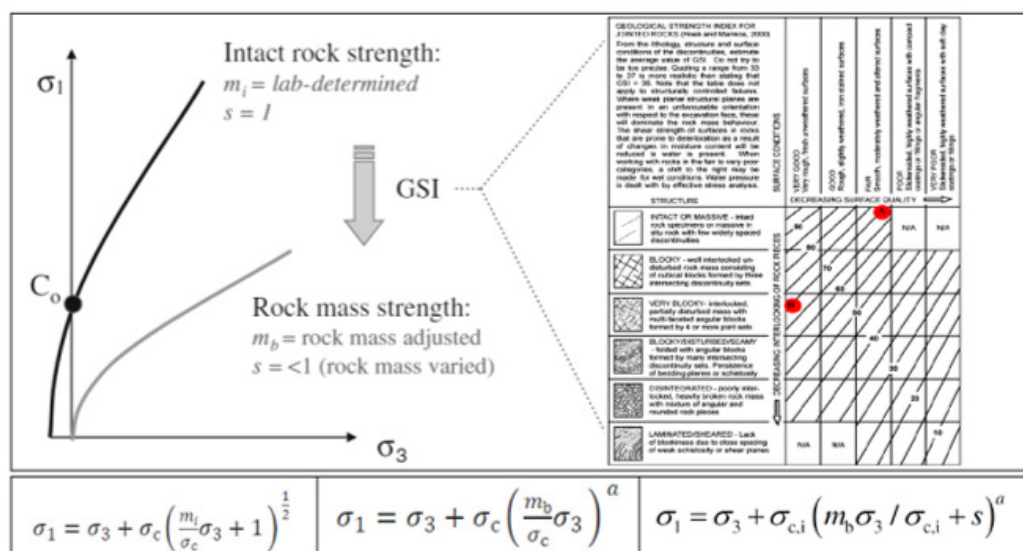


**Figure 3:** A convenient summary of the Hoek-Brown intact rock and 'rock mass' criteria, indicating reduced GSI for reduced 'rock mass' strength. Expanding the right-hand side one can note the instructions in small print from Hoek, that are ignored by most users when anisotropic rock masses are present.

The GSI-rating selection scheme shown in Figure 3 is based on a brief encounter with 'geology' (the sketches) followed by what could truly be called black-box modelling. With reference to the (Bieniawski) x-axis on the GSI chart, why does slickensiding have to be 'highly weathered' and with clay-filling? Why cannot rougher joints have clay filling and be weathered as they of course can be in reality, and in the Q-system? GSI is actually the least 'geo-logical' method in use in rock engineering. Yet it is used by thousands since 'simple'.

One may wonder why the profession has adopted a modified intact rock strength equation and assumed it applies to rock masses which are so very different from the numerous but very small intact rock triaxial test samples of approximately 30 cm<sup>3</sup> volume that were utilized in the original (and genuinely empirical) intact rock criterion. The writer had always assumed that the lab-determined

$m_i$  was an important part of the intact rock H-B strength criterion. Recently, the range of  $m_i$  for sandstone is reported to be from 4 to 35, for limestone from 4.5 to 40, for shale 3.7 to 25, for slate 1.4 to 31, and for gneiss 5.3 to 32 [4]. One can then wonder if  $m_b$  (see Figure 2) is also only poorly linked to rock type. Despite this, GSI use continues world-wide.

The Hoek instructions about 'homogeneity' given in the Figure 4 caption can never apply to the Q-system since rock masses are often anisotropic [5], therefore starting with RQD (used for core logging). The usually anisotropic rock mass structure's least favourable pair of  $J_r$  and  $J_a$  is applied to the least favourable joint set or clay-filled discontinuity when evaluating the simple equation for Q. (Note that RQD/ $J_n$  represents relative block size, and  $\tan^{-1} J_r/J_a$  represents inter-block frictional strength):

$$Q = RQD / J_n \times J_r / J_a \times J_w / SRF \quad (2)$$



**Figure 4:** Note Hoek's own figure caption from Hoek and Diederichs, [15] which is an article about deformation modulus. 'Road cut in which the size of individual rock blocks is of the same order as the height of the cut. Rock mass classifications, based on the assumption of homogeneity, cannot be applied to this rock mass'. This Hoek advisory emphasises the gulf between GSI and the intended use of the Q-system which is obviously used to address just such rock masses, which are common, also in tunnelling. Refer to Figures 5 and 6 to see further problems.

|   |     |  |
|---|-----|--|
| $GSI_1 = RMR_{1989} - 5 = R_1 + R_2 + R_3 + R_4 + R_5 (=15) - 5$                        | (1) | Hoek et al. 1995                         |
| $GSI_2 = 1.5 R_4 + 0.5 RQD$   | (2) | Hoek et al. 2013                         |
| $GSI_3 = 15 \log \left( \frac{RQD}{J_n} \frac{J_r}{J_a} \right) + 50$                   | (3) | (This was not a Barton, 1995 suggestion) |
| $GSI_4 = 9 \ln \left( \frac{RQD}{J_n} \frac{J_r}{J_a} \right) + 44$                     | (4) | Hoek et al. 1995                         |
| $GSI_5 = \frac{52 J_r / J_a}{(1 + J_r / J_a)} + 0.5 RQD$                                | (5) | Hoek et al. 2013                         |
| $GSI_6 = \frac{26.5 + 8.79 \ln J_c + 0.9 \ln I/b}{1 + 0.0151 \ln J_c - 0.0253 \ln I/b}$ | (6) | Cai and Kaiser 2006                      |
| $GSI_7 = 153 - \left[ \frac{165}{1 + \left( \frac{J_p}{0.19} \right)^{0.44}} \right]$   | (7) | Russo 2009                               |

**Figure 5:** Attempts to improve the quantification of GSI by Hoek and others. It is not clear what would be the consequences for 'c' and ' $\phi$ ' in Figure 2 as the parameters that Hoek has selected, many from the Q-system (equation 2) are themselves subjective.



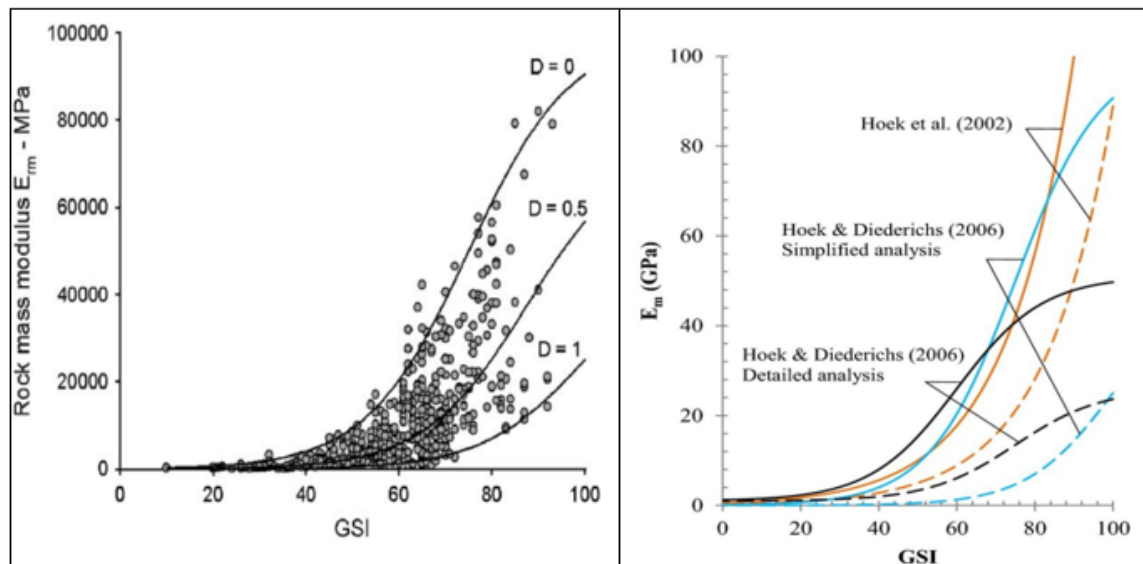


**Figure 6:** The widely varying deformation modulus estimates connected with GSI. The left-hand figure shows test data from Taiwan and China given by Hoek and Diederichs [15]. The right-hand figure is from Renani & Cai [16]: Forty-Year Review of the Hoek–Brown Failure Criterion for Jointed Rock Masses. It appears that GSI is not a reliable parameter for making such estimates. But it is used by thousands.

One may seriously ask how continuum modelers are choosing deformation modulus. Perhaps by waiting for the results of the modelling and adjusting the disturbance factor  $D$ ? Several private communications to the writer have stated such, and if this is so it seems hardly a defensible method for developing and presenting modelling results to a client.

### The Contrasting Worlds of Continuum and Discontinuum Modelling

A good introduction to the contrasts is given by the Figure 7 modelling results, which were produced before GSI existed. Both modelling methods: FLAC and UDEC are the result of Peter Cundall's important developments, marketed successfully by Itasca.

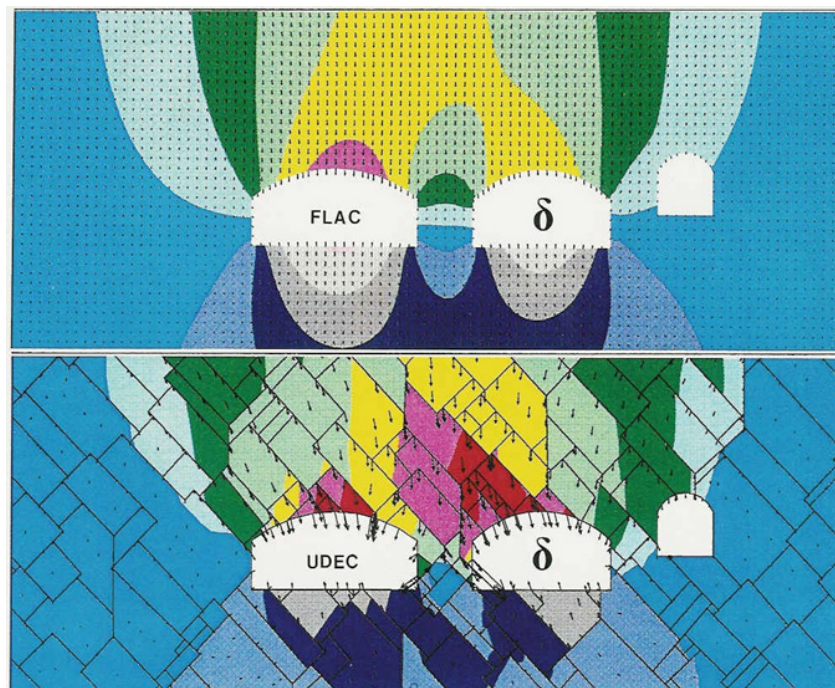


**Figure 7:** Comparison of FLAC and UDEC-BB by a former colleague Lise Backer. The same triple-tunnel motorway is modelled using the same boundary stresses and the same intact-block deformation moduli. The jointing makes the UDEC-BB model significantly more realistic than the continuum model. Marked anisotropy can be noted, and pillar distress can be seen when looking closely.

Many designers have been using continuum modelling for their tunnel studies. Most have presumably accepted that when their models plot plastic zones, they need to take note and perhaps suggest longer rock bolts. (Usually not correct but understood). In fact the Rocscience modelling package of Phase 2 FEM (today RS2) using GSI and H-B formulations (Figure 2) was proved in an international court case to be providing grossly exaggerated 'plastic' zones. These were claimed to be of 10m to 14m diameter in

relation to a 3.5m span pressure tunnel which was driven for 7km without the need for shotcrete support. The court case arose due to a claim against the contractor for 'an insufficiently supported' tunnel. In fact, only the invert had been damaged by a much too fast drainage (20m/hour) when those monitoring strains in the penstock became worried and asked for fast emptying. Six nations were involved in this landmark court case. Figure 8 suggests how to select more appropriate modelling methods.

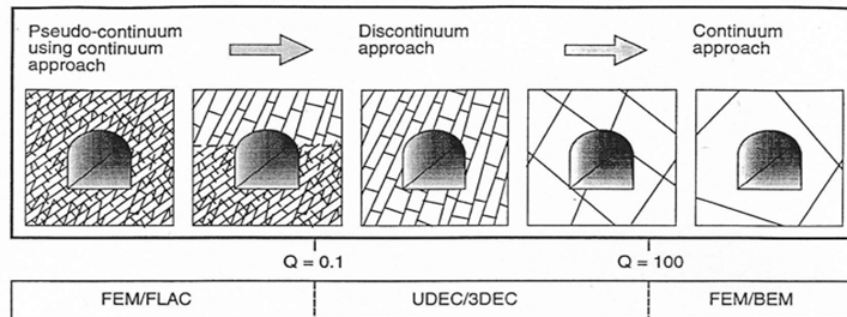


**Figure 8:** An approximate Q-value based scheme for choosing the broadly appropriate type of modelling techniques. In the opinion of many, 90% of rock masses need discontinuum treatment. Realistic modelling requires greater attention to the details of jointing than when using GSI, Hoek-Brown and continuum modelling. Figure 9 illustrates some of the problems with continuum modelling and use of M-C or H-B concepts.

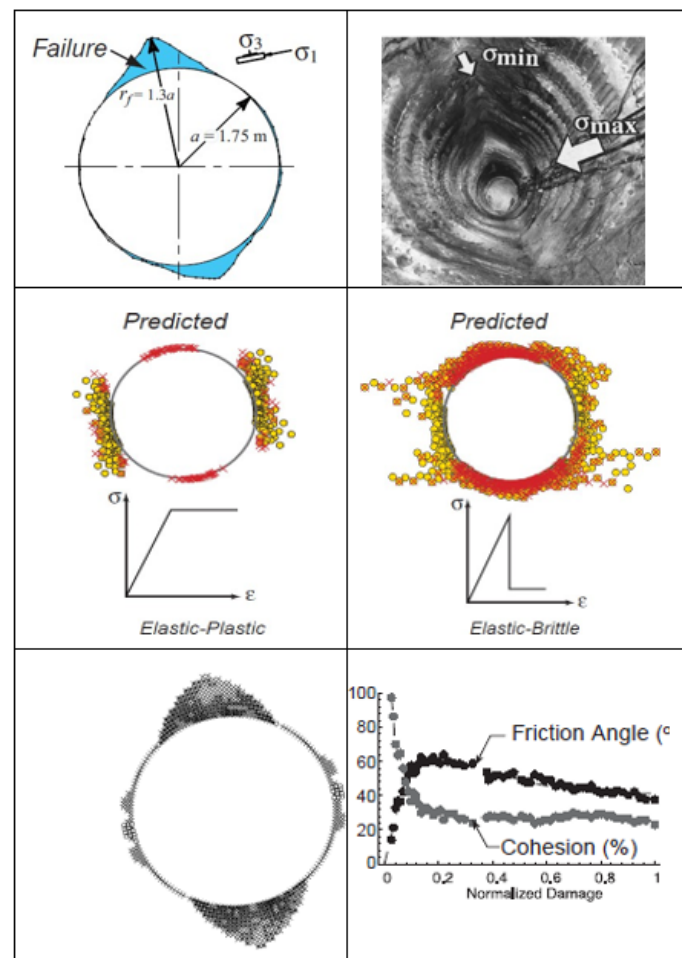


**Figure 9:** The inability of standard continuum modelling routines with M-C or H-B to capture reality is nicely illustrated in the central diagrams. So-called cohesion softening and friction hardening (CSFH third row) is seen to be doing a far better job despite the continued continuum modelling, here with Cundall's FLAC. Hajiabdomajid et al. [17].

It is in fact the continuum modelling of rock slopes that most clearly reveals the incorrect nature of the GSI H-B modelling scheme because there is visual evidence of reality which is mostly 'hidden' around tunnels. The problem is the thousands of published but hardly ever observed 'circular' or 'spoon-shaped' failures that the modelers presumably feel comfortable with since rock mechanics literature is full of such. Reality is usually different, with joint sets

and faults being involved and the possibility of monitoring the usually progressive actual failures. Rock masses do not fail 'with the click of a finger' suggested by the Mohr-Coulomb or Hoek-Brown addition of the 'c' and ' $\sigma_n \tan \phi$ ' components, linear (M-C) or non-linear (H-B). Let us examine an extract from a well-written (but continuum-based) keynote paper: Figure 10.

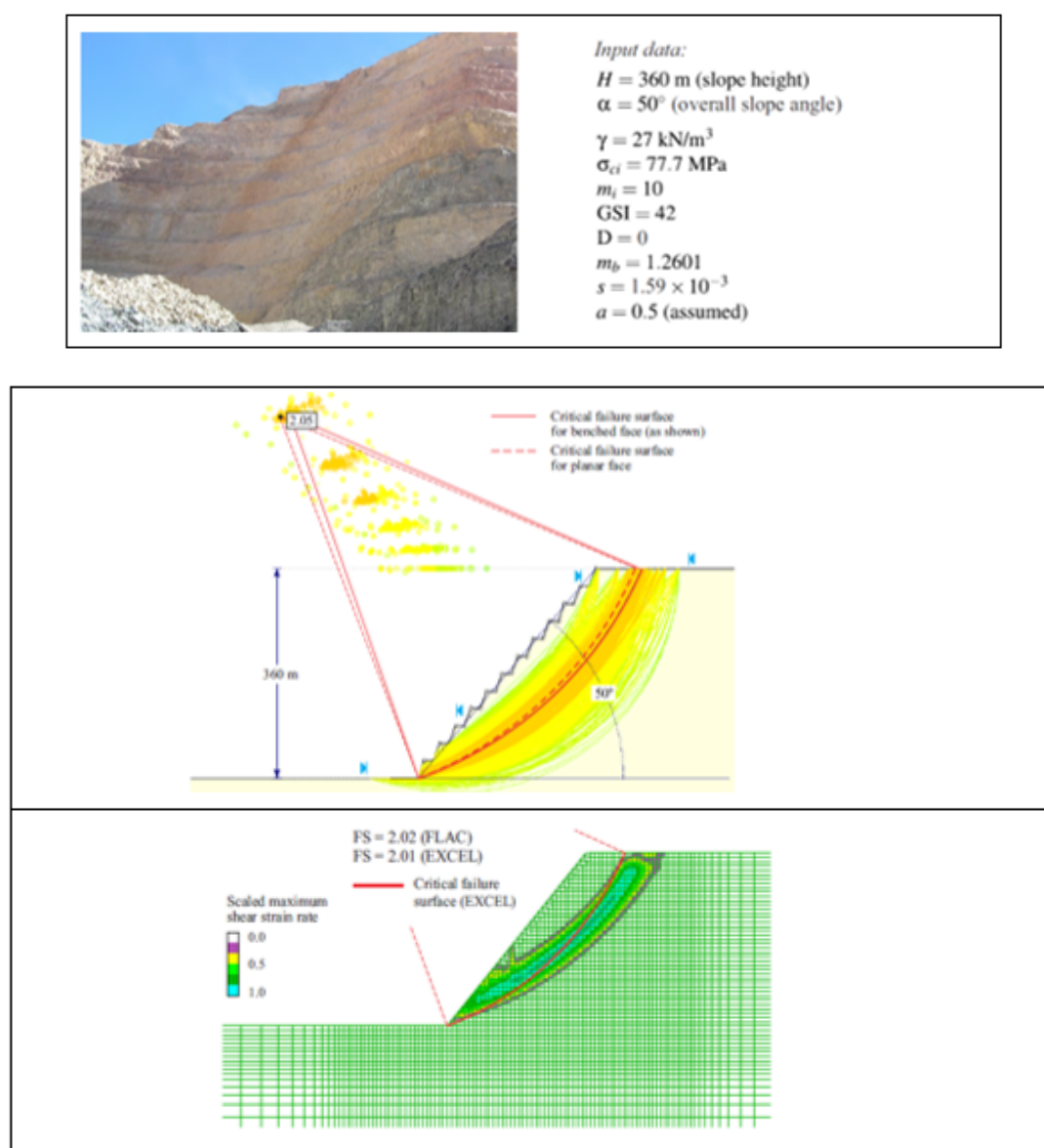


**Figure 10:** Computations with continuum codes SLIDE and FLAC of the steep open pit slope that is given the competent rock (UCS = 78MPa) GSI Hoek-Brown based input data shown next to the photo. Reproduced from the keynote lecture given by Carranza-Torres, 2021. He assumes 'Hoek-Brown' behaviour here, but this is actually only relevant for very weak or disintegrated media like rockfill or soil. Numerous 2D 'spoon' shaped failure predictions are presented. A worrying GSI H-B myth is promoted. Photographs of apparent 'circular' failures that Carranza-Torres also shows are in 'saprolite' or 'lake-bed sediments' and one actually involves a major fault.



A more recent strain-softening model that includes cohesion weakening and frictional hardening (CSFH) is the Itasca Model for Advanced Strain-Softening (IMASS) introduced by Ghazvinian et al. 2020. IMASS was developed to represent a weak rock mass's response to stress changes (i.e., rock mass yield, modulus softening, density adjustment, dilation, cohesion weakening, and frictional strengthening). A basic assumption is that the peak strength envelope is similar to the post-peak envelope for the case of very weak rock masses. In other words, it is assumed that the rock mass is already damaged, resulting in ductile behavior. A shear strength equation for rockfill [6] is incorporated. The IMASS model is being increasingly implemented where large strain and ductile behavior is expected in the case of open pits with poor rock mass conditions (e.g. Cacino et al. [7]).

### Discontinuum Modelling when this is more Appropriate

A recent study of open-pit failures from many countries by Kolapo et al. [8] has shown a great dominance of discontinuity or joint related causes. Their compilation, which is reproduced in Figure 11, has only been modified by highlighting the cases where natural joints or faults or shear zones are not specifically reported. Perhaps the first case should also have been highlighted.

In Figure 12 'stills' are reproduced from a drone video sequence that helps to illustrate the very frequent presence of joints and/or faults that are usually registered when open-pit slope failures are investigated. Figure 13 caption shows slope height-angle data from an open pit which also had steep joints.

Presence of tension crack formation, crack widening and extension  
 Multiple failures occurred as a result of intersection of discontinuities  
 Intersection of joint sets  
 Presence of shear zones, faults and sets of discontinuities  
 Steeply dipping joints, increase in groundwater pressure and melting of snow  
 Groundwater condition, Steeply dipping faults  
 Structural discontinuities, precipitation, run off, poor quality and low strength rock mass  
 Large fault zone passing through a weaker rock mass  
 Intersection of several thick shear zones and smaller scale discontinuities  
 Steeply dipping joint sets and faults  
 Presence of faults and joints  
 Increase in water level, poor geological structure and continuous rainfall  
**Heavy rainfall**  
 Presence of fault zones  
**Presence of tension cracks, heavy rainfall, groundwater pressure**  
**Presence of tension cracks**  
 Rise in water table, fractured rock mass with minor joints and larger fault structure  
 Presence of wider fault zones and clay infillings  
 Presence of steeply joint sets  
 Intersection of joint sets  
 Intersection of faults, presence of clay gouge in fault zones  
 Presence of flat sipping fault, High water pressure  
 Numerous faults and several joints  
 Presence of faults and set of joints  
 Presence of set of joints

**Figure 11:** A comprehensive record of the mostly joint and discontinuity caused reasons for open pit failures. Very few cases without structure are listed. From: An overview of slope failure in mining operations. Kolapo et al. [8]. Mining Journal.

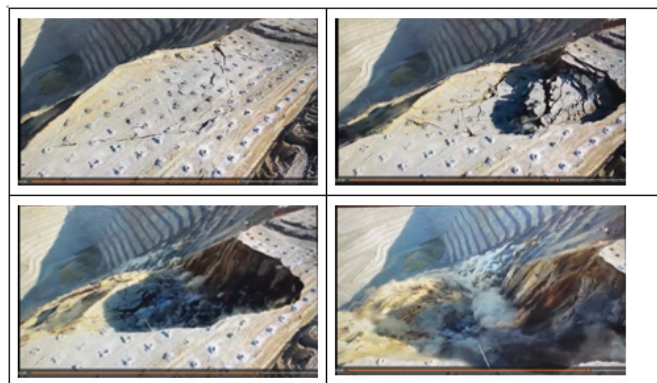
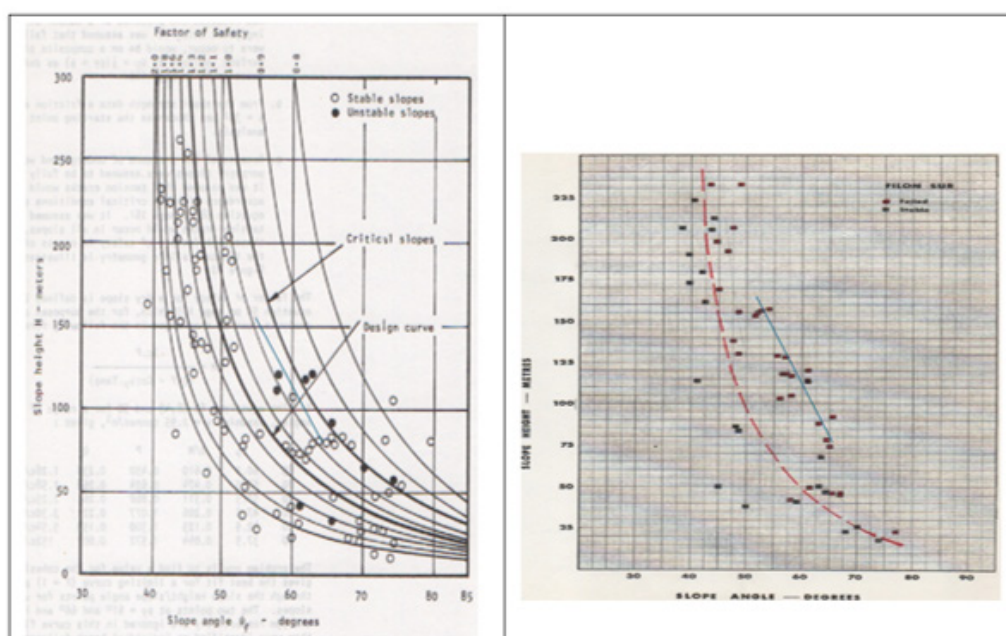






Figure 12. Drone photos at 4-, 5-, 7-, and 17-seconds intervals showing the presence of adversely dipping joint sets which obviously played their part in this smaller slope failure at Bingham open-pit.  
<https://www.youtube.com/watch?v=YPhDAXt-hU>. A massive failure at this pit ten years ago involved an adversely dipping fault plane of several 100's of meters length and width down-dip.



**Figure 13:** Historic slope-height slope-angle data from Hoek and Bray [20] here supplemented by many more cases (>30) of failed slopes in Rio Tinto's old Filon Sur pit in altered porphyries, from Barton [21]. Two steeply dipping (to SW and SE) joint sets were present behind the north wall failures, resembling the Bingham failure shown in Figure 12.

In Figure 14 the two principal stress-deformation components for rock joints that differentiate discontinuum from continuum modelling are shown. The very frequent presence of rock joints, in fact sets of intersecting rock joints, is what often differentiates the reality from the GSI-based assumption of homogeneity with no joints modelled once the GSI value is chosen (Figure 3) and ambiguous H-B equations are 'mobilized' in FEM.

The normal stress-closure curves (N) for real rock joints shown in Figure 14 are from Bandis et al. 1983, and the shear stress-displacement curves (S with scale effects) are from Bandis et al. [9]. The N, N+S and S load-deformation trends for the three imaginary

'plate-loaded' rock mass assemblies are from Barton, 1986.

Chryssanthakis et al. [10] matched the three styles of deformation using UDEC-BB after this code became available in 1985. The relative lack of shear (left), combined shear and closure (N+S) for the basalt columns, and greatly dominating shear (S) in the case of the conjugate jointing serve as illustration of serious differences between what we learn from discontinuum and continuum codes. The concave, linear and convex P vs  $\Delta$  modes have each been recorded in large-scale plate-loading or flatjack-loading in situ tests in tunnels [11].

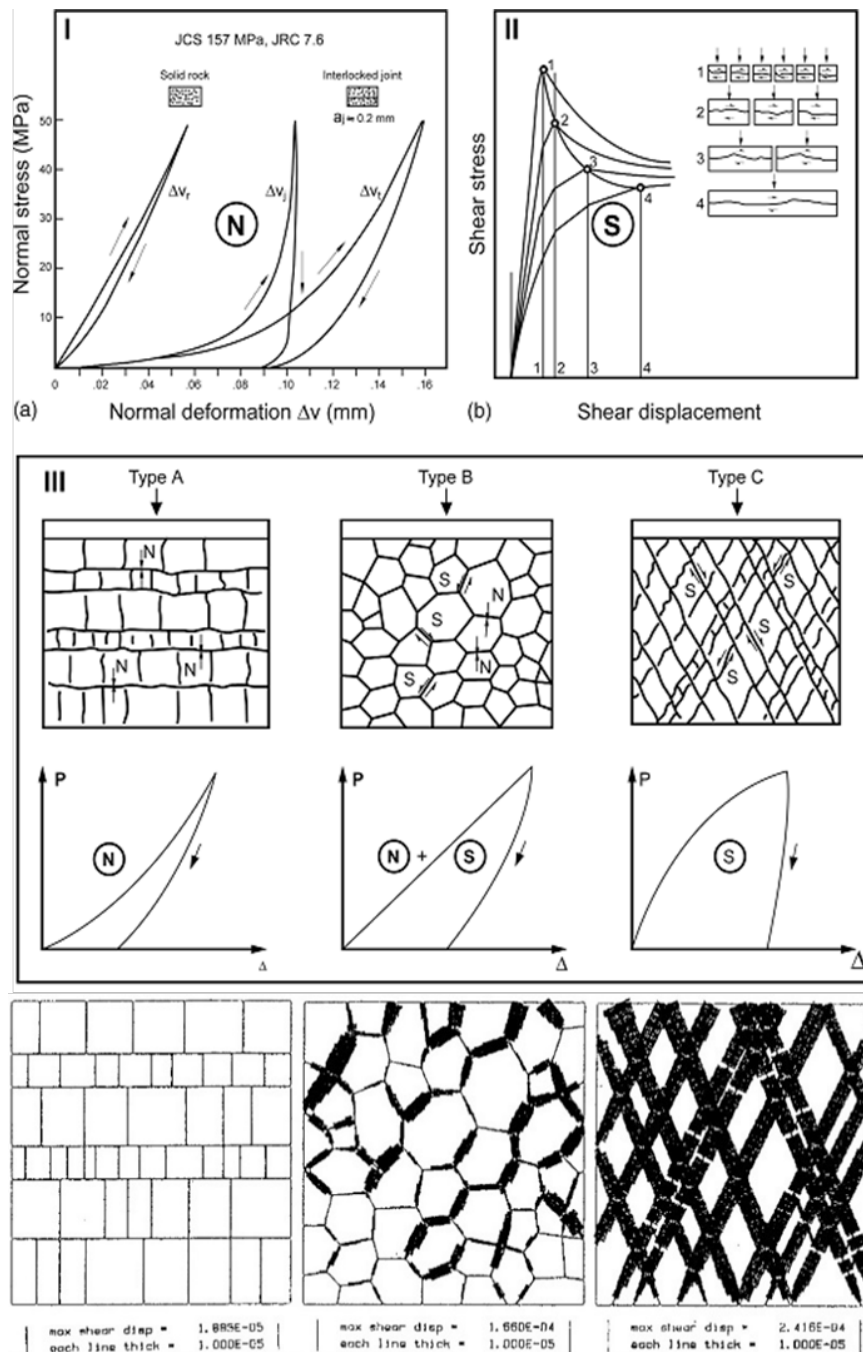


**Figure 14:** The N (normal) Type A concave deformation and the S (shear) Type C convex deformation, with the combined mode Type B as seen in loading tests across columnar basalt. Note the increasing shear component from left to right. In the next section and in Figure 15 we explore more of the 'S' component, but expressed as shear strength versus normal stress, these strength envelopes having convex forms but with different steepness.

### Realities of Progressive Failure: Rock Mass Shear Strength Components

It would not be possible to monitor a potential rock slope failure, as is common practice in large open-pits, if Mohr-Coulomb or Hoek-Brown had been relevant models. These widely used methods represent shear failure assuming 'click-of-the-fingers simultaneous 'c plus  $\sigma \tan \phi$ ' mobilization and are the source of major errors in

our subject. Perhaps they are appropriate for soil, sand or rockfill. Shear failure in rock masses is actually process-dependent, because it is shearing strain / shear displacement dependent, as described in four stages in the Figure 15 caption.

The Barton-Bandis shear strength criterion in UDEC-BB has displacement dependent mobilization and degradation of JRC, and corresponding adjustment of physical and hydraulic joint

apertures. It also has built-in scaling of shear strength in relation to block size – specifically the spacing of cross-jointing for the relevant joint set. Figure 16 is an example of UDEC-BB application for design checks of the Gjøvik cavern of 62m span. We see the wide ‘top-heading’ (excavation stages 1 through 5) and the well-controlled deformation assisted by quite high horizontal stress. Seven MPBX

extensometers showed maximum deformations in the 7 to 8mm range, almost identical to the modelling. The location of the cavern on the Q-system support chart of 1993 developed by Grimstad is shown in Figure 17. See Barton et al. [1] for the details of tunnel and cavern Q-based support and its updating.

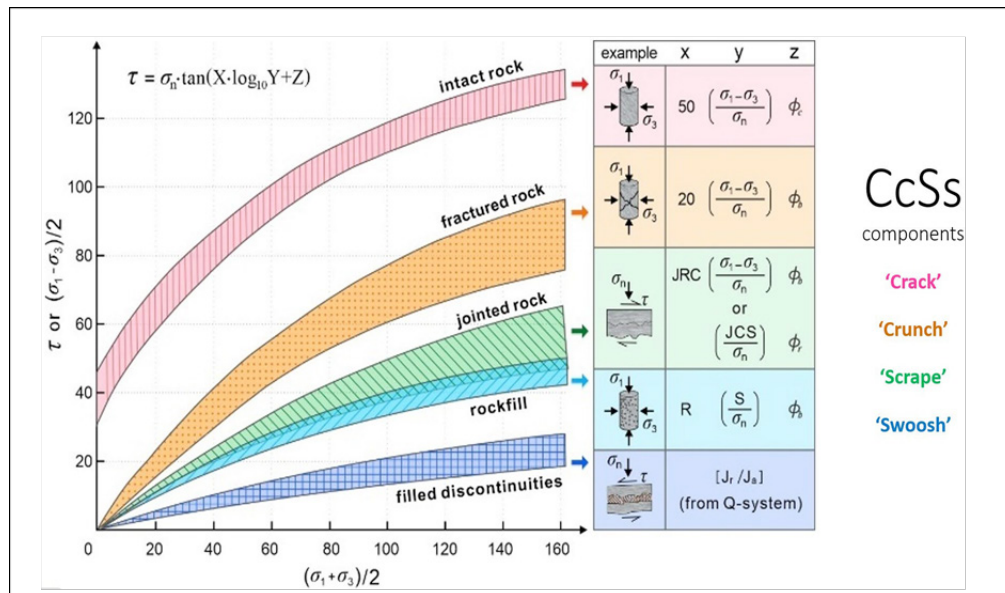


**Figure 15:** The components of shear strength of rock masses CcSs, here represented as laboratory test ‘examples’ for purposes of illustration only: 1. Pink intact rock bridges will be the stiffest and fail first: ‘C’ for ‘crack’. 2. These new orange fracture surfaces with highest JRC, JCS (= UCS) and  $\phi_b (> \phi_r)$  are next stiffest and fail next ‘c’ for ‘crunch’, followed by 3. shear mobilization along green capable joint sets: ‘S’ for ‘scrape’, followed by shearing 4. on blue clay-filled discontinuities: ‘s’ for ‘swoosh’ if such are present. One can imagine these components being activated in the Figure 12 sequence. After Barton [23].

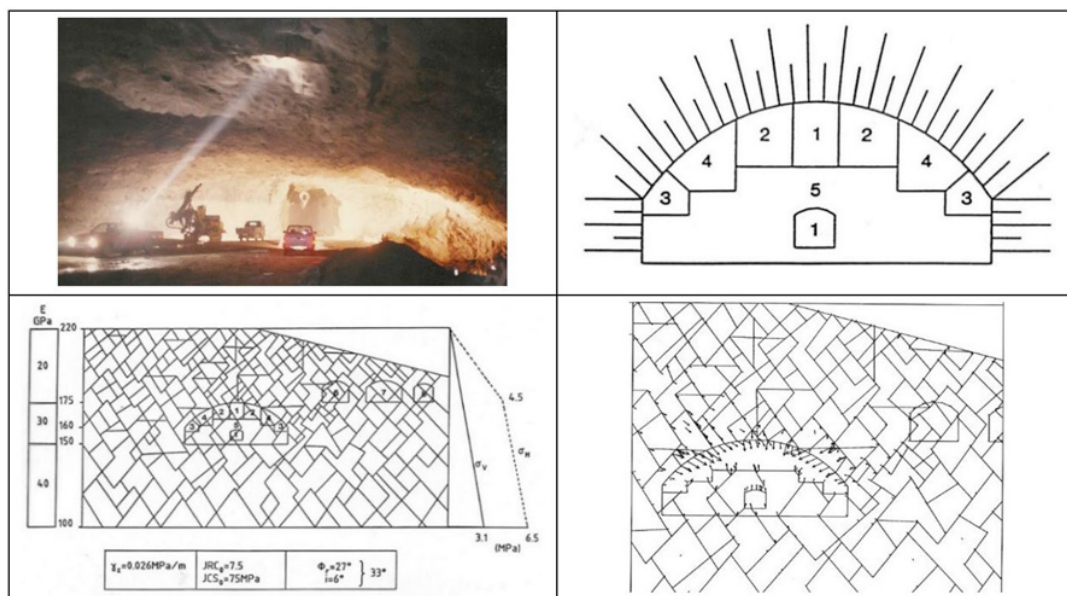


**Figure 16:** Gjøvik Olympic cavern of 62m span: top-heading, rock reinforcement, excavation stages with input data and part of the UDEC-BB modelling. Barton et al. [24].



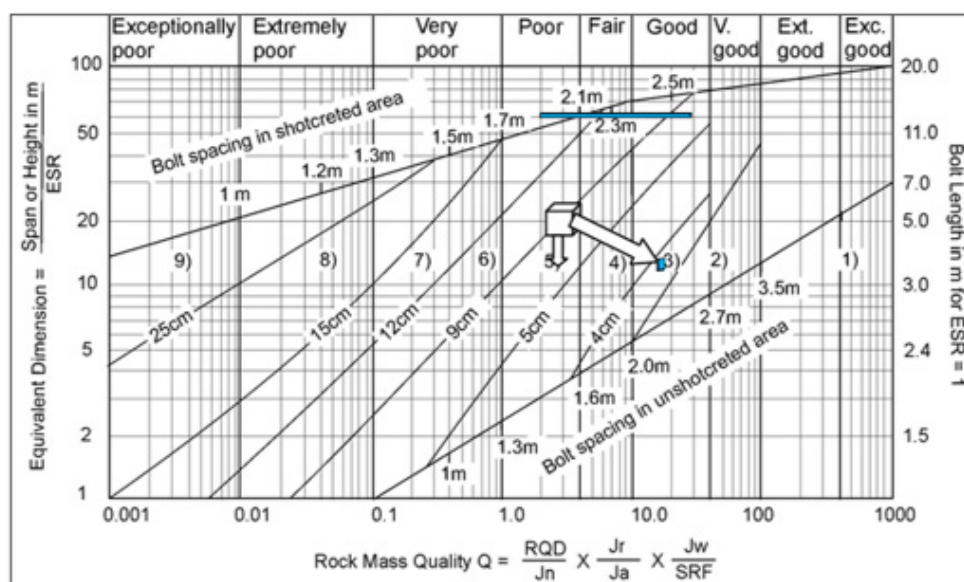


**Figure 17:** The Q-system tunnel and cavern support and reinforcement chart of 1993. The thin blue line shows the range of  $Q = 2$  to  $30$  for the 62m span cavern. B 2.5m c/c + S(fr) 10cm based on  $Q_{\text{mean}} = 10-12$ ,  $Q_{\text{range}} = 2$  to  $30$ . (RQD was 60 to 90).

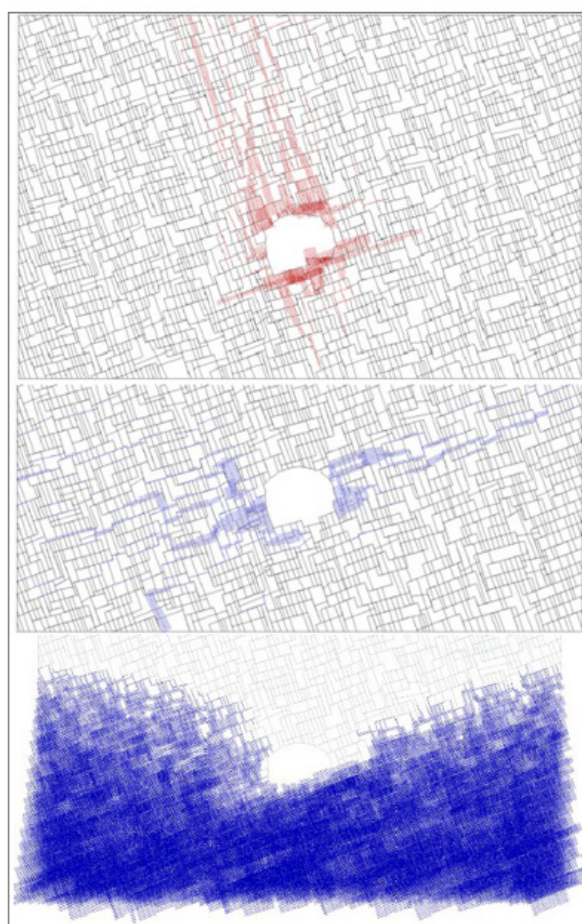


**Figure 18:** UDEC-BB modelling which was used in a court case concerning the consequences of failure to pre-inject a metro tunnel in jointed granites. Priv. comm. Dr. Karstein Monsen. Some of the basic details of coupled joint modelling were given in Barton, Bandis and Bakhtar [22].

A result which can be obtained with distinct element modelling but obviously not with continuum modelling is illustrated in Figure 18. It depicts UDEC-BB modelling of a metro tunnel that should have been pre-injected by the contractor. Principal shearing (red) and inflow (blue) are shown on different joint sets due to JRC differences causing lower shear strength, or larger joint apertures respectively. A wedge in the floor is removed so that the locally outsize deformation and inflows do not disturb the graphics. The dark blue is of course drawdown of the modelled water in the two joint sets. Models that give valuable insight obviously take much longer than Figure 7a.

## Conclusions

- a. Unfortunately, and surprisingly the simple but misleading GSI number for 'rock mass quality' (the 'geological strength index') appears respectively 16, 12 and 10 times in the Hoek-Brown equations for the presumed shear strength of rock masses for 'c' and ' $\phi$ ' and ' $\sigma_{cm}$ '. This is because of the three supporting equations for mb s, and a. These include the disturbance factor D, which is poorly quantified yet also appears 7 and 6 times in the H-B equations for presumed rock mass 'c' and ' $\phi$ '.
- b. It means presumably that errors of judgement in selecting an appropriate GSI value (and D value) will be amplified in the estimates of H-B 'c', ' $\phi$ ', ' $\sigma_{cm}$ ' and 'Em.' The latter has no adjustment for depth or stress level so is often incorrect.
- c. Rock masses are most often jointed and faulted and anisotropic so modelling as if isotropic continua is a highly suspect approximation. An international court case has proved that the GSI, H-B, FEM modelling that is used by so many exaggerates the dimension of yield zones commonly known as 'plastic zones'.
- d. It is well known by those with slope stability experience in open pit mines that unless the rock is extremely weak or intensely fractured and altered or weathered it does not fail in the form of circular or spoon shaped surfaces. Capable joint sets perhaps with individual fault planes as relief surfaces are the most common form of failure and major wedge failures tend to dominate as a result.
- e. The simultaneous addition of 'c' and ' $\sigma_{n \tan \phi}$ ' as in classic linear Mohr-Coulomb, and in non-linear Hoek-Brown is basically an erroneous calculation method because the cohesive component has higher stiffness and attracts the highest shear stresses and fails first, if at all. This is followed by mobilization of friction. Cohesion softening and friction hardening CSFH is fundamentally more correct, but a more comprehensive model that allows for true progressive failure is CcSs.

## References

1. Erharther GH, N Bar, TF Hansen S Jain, T Marcher (2024) International Distribution and Development of Rock Mass Classification: A Review. *Rock Mechanics and Rock Engineering*.
2. Barton N, E Grimstad, R Abrahão, N Bar (2024) Celebrating 50 years of Q system development for infrastructure design and follow-up. *Proc. ISRM symp. New Delhi, Keynote lecture pp. 37.*
3. Barton N (1973) Review of a new shear strength criterion for rock joints, *Engineering Geology, Elsevier, Amsterdam* 7: 287-332.
4. Davarpanah SM, Sharghi M, Vasarhelyi B, Á Török (2022) Characterization of Hoek-Brown constant mi of quasi-isotropic intact rock using rigidity index approach. *Acta Geotechnica* 17: 877-902.
5. Barton N, E Quadros (2015) Anisotropy is everywhere, to see, to measure and to model. *Rock Mechanics and Rock Engineering* 48: 1323-1339.
6. Barton N (2008) Shear strength of rockfill, interfaces and rock joints and their points of contact in rock dump design. Keynote lecture, Workshop on Rock Dumps for Mining, Perth.
7. Cancino C, L Lorig J Bu, N Bar (2024) Back-analysis for more reliable mine plans at Pueblo Viejo Gold Mine. *Slope Stability, Belo Horizonte, Brazil* pp. 13.
8. Kolapo P, G Oniyide KO Said, AI Lawal, M Onifade (2022) An overview of slope failure in mining operations. *Mining Journal* 2(2): 350-384.
9. Bandis S, Lumsden A, Barton N (1981) Experimental studies of scale effects on the shear behaviour of rock joints. *Int. J. Rock Mech Min Sci and Geomech Abstr* 18: 1-21.
10. Chryssanthakis P, Monsen K, Barton N (1991) Tunnelling in jointed rock simulated in a computer. (In Norwegian). *Tunneller og Undergrunnsanlegg, NTNF, Oslo* pp. 23-28.
11. Barton N (1986) Deformation phenomena in jointed rock. 8th Laurits Bjerrum Memorial Lecture, Oslo. *Geotechnique* 36(2): 147-167.
12. Bieniawski ZT (1989) *Engineering Rock Mass Classifications: A Complete Manual for Engineers and Geologists in Mining, Civil, and Petroleum Engineering*, New York, Wiley pp. 272.
13. Hoek EC, Carranza Torres, B Corkum (2002) Hoek-Brown failure criterion – 2002 Edition. *Proc. NARMS-TAC Conference, Toronto* 1: 267-273.
14. Müller L (1966) The progressive failure in jointed media. (In German). *Proc. of ISRM Cong, Lisbon* 3(74): 679-686.
15. Hoek E, MS Diederichs (2006) Empirical estimation of rock mass modulus E. *International Journal of Rock Mechanics & Mining Sciences* 43: 203-215.
16. Renani HR, M Cai (2021) Forty-Year Review of the Hoek-Brown Failure Criterion for Jointed Rock Masses. *Rock Mech. and Rock Eng* 55(4):1-23.
17. Hajiabdomajid V, CD Martin, PK Kaiser (2000) Modelling brittle failure. *Proc. 4th North American Rock Mechanics Symposium, NARMS Seattle* J Girard, M Liebman, C Breeds, T Doe (Eds.), pp. 991-998.
18. Carranza Torres C (2021) Computational tools for the analysis of circular failure of rock slopes. Keynote Lecture. In *Proceedings of EUROCK 2021, Torino, Italy*.
19. Ghazvinian E, Garza Cruz T, Bouzeran L, Fuenzalida M, Cheng Z, et al. (2020) Theory and Implementation of the Itasca Model for Advanced Strain Softening (IMASS). *MassMin (2020), Proc 8th Int Conf & Exhib. on Mass Mining, Virtual Conference, Santiago, Univ of Chile*, pp. 451-461.
20. Hoek E, JW Bray (1976) *Rock Slope Engineering*. Institution of Mining and Metallurgy. 2<sup>nd</sup> Edition, pp. 402.
21. Barton NR (1971) A model study of the behaviour of steep excavated rock slopes. PhD thesis, Imperial College, Univ of London, UK pp. 377.
22. Bandis S, Lumsden AC, Barton N (1983) Fundamentals of rock joint deformation. *Int J Rock Mech Min Sci and Geomech. Abstr* 20(6): 249-268.
23. Barton N (1999) General report concerning some 20th Century lessons and 21st Century challenges in applied rock mechanics, safety and control of the environment. *Proc. of 9th ISRM Congress, Paris, Balkema, Netherlands* 3: 1659-1679.
24. Barton N, By TL, Chryssanthakis P, Tunbridge L, Kristiansen J, et al. (1994) Predicted and measured performance of the 62m span Norwegian Olympic Ice Hockey Cavern at Gjøvik. *Int J Rock Mech Min Sci Geomech Abstr* 31(6): 617-641.